Structural Characteristics of a Copper-Nickel Alloy Obtained by Selective Laser Smelting

To cite this article: V V Baraz *et al* 2020 *IOP Conf. Ser.: Mater. Sci. Eng.* **971** 032053

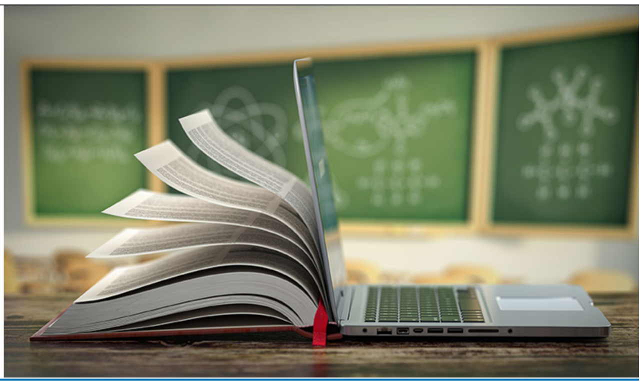

IOP Conf. Series: Materials Science and Engineering **971** (2020) 032053 doi:10.1088/1757-899X/971/3/032053

Structural Characteristics of a Copper-Nickel Alloy Obtained by Selective Laser Smelting

V V Baraz, S S Gerasimov and I A Gruzdeva*

Ural Federal University named after the first President of Russia B.N. Yeltsin, Ekaterinburg, Russia

*i.a.gruzdeva@urfu.ru

Abstract. A three-dimensional model from powders of a copper-nickel alloy Cu81-Ni19 composition is obtained by selective laser smelting. The 3D model microstructure is characterized by the absence of typical crystalline structure and contains elements of a quasi-amorphous state. The finished material differs from the standard monolithic cast billet with a lower surface roughness, higher hardness values while maintaining almost the same density indices.

1. Introduction

Additive manufacturing (3D printing) is a promising technological process, its main principle is the functional products formation through layer-by-layer growing of a volumetric object [1-3]. Selective laser smelting (SLS) is one of the most common additive technologies that allow you to create metal products from the powder substance by melting using high-energy laser radiation. Thus, the traditional technology based on the removal of the primary material (by machining - milling, turning, etc.) can be supplemented by the opposite method - the gradual addition of material and filling it to the desired shape.

At present, additive technology is being successfully implemented with respect to a wide group of various materials, including metals and alloys [4, 5]. Among the latter, some non-ferrous metals and their alloys should be noted [6, 7]. Moreover, the practical use of selective laser smelting technology as applied to alloys of the Cu-Ni system, which are used not only for industrial purposes, but also in the field of creating artistic and decorative articles, may be of independent interest.

The aim of the study was to use the SLS method to obtain a three-dimensional object made of a copper-nickel alloy of the Cu81-Ni19 composition.

2. Material and research methods

The chemical composition of the MH19 alloy was (mass. %): 19.06 Ni, 0.157 Fe; 0.245 Si; the rest is Cu.

Powder for 3D printing was made by flame spraying. To prepare the powder, a wire billet with a diameter of 0.8 mm made of the same composition alloy was used as a starting material. After drying the powder fractions by means of a laboratory separator LPzE-2e, a powder with a particle diameter of not more than 40 μm was obtained. The manufacture of three-dimensional 3D-models was carried out on an industrial installation EOS M280. The laser power is 200 W, the diameter of the laser spot is 100 μm, the deposition thickness of powder monolayers is 20 μm. The formation of the 3D-model was carried out on the workpiece, that was cut from deformed by rolling and then annealed plate. The workpiece was made of the same composition alloys and its dimension was 30x30x10 mm. The density ρ was measured by hydrostatic weighing using a METTLER TOLEDO analytical balance. Microhardness tests were carried out by the standard method on a PMT-3 instrument with a load of 50 g (0.5 N). The surface roughness was evaluated on an Optical profiling system Veeco WYKO NT1100 optical profilometer. The structure was studied using an Epiquant automated metallographic microscope and a ZEISS CrossBeam AURIGA scanning electron microscope.

3. Experimental results and discussion

The results of the structure metallographic study of the sintered billet after laser smelting (3D model) are shown in Fig. 1. The sample structure made by SLS method has a form that differs fundamentally from the classical structure of cast article had a face-centered cube lattice. The cast sample structure is distinguished by the presence of clear grain boundaries and wide bands of annealing twins [8]. The 3D model structure consists of numerous dispersed fragments, which have a characteristic form of the so-called turbulent eddies, preserving a drop-like configuration [9]. These structural fragments size falls within the range of 70-100 μm.

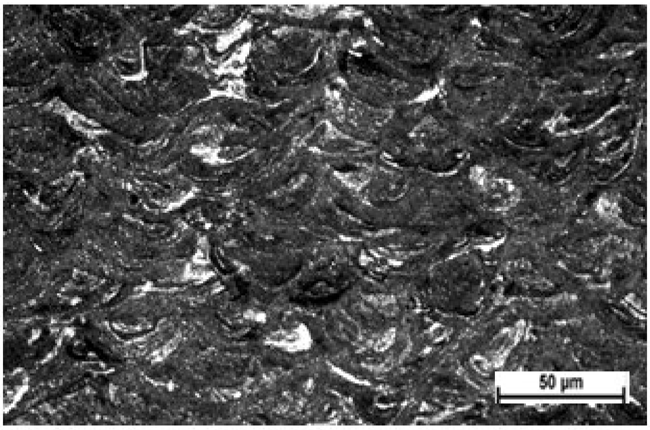

Figure 1. The structure of the Cu81-Ni19 alloy made by selective laser smelting

Thus, a metallographic assessment of the sample structural state obtained by laser smelting does not allow us to detect the usual characteristics of a metal material that has undergone crystallization. There are no dendritic formations; there are no elements of the grain structure with the presence of the boundaries of these structural objects.

There is an assumption that under conditions of local laser heating, subsequent cooling in the molten sections proceeds at such a rate that it becomes possible to suppress the crystallization process and fix the strongly supercooled liquid phase, i.e. obtaining an amorphous state (metal glass).

As an explanation, a diagram is given (Fig. 2), which interprets the conditions for obtaining such a structural state in the case of deep supercooling of the liquid phase. As is known [9], the temperature dependence of the crystallization rate curve is described by an extremal curve characterized by the position of the kinetic maximum in the region of average supercooling temperatures. The indicated position is due to the uneven effect of the cooling temperature on the indices of thermodynamic and kinetic factors. On the one hand, if the temperature decreases, i.e. the degree of supercooling is enhanced, the role of the difference in free energies between the supercooled liquid phase and the emerging crystalline phase is also enhanced. On the other hand, the diffusion influence is suppressed. If rapid (ultrafast) cooling is ensured from the initial (equilibrium) state (temperature T_0), bypassing temperature T_1, up to temperature T_2, the crystallization is suppressed and a strongly supercooled (frozen) liquid phase (metal glass) is formally fixed at a low (room) temperature.

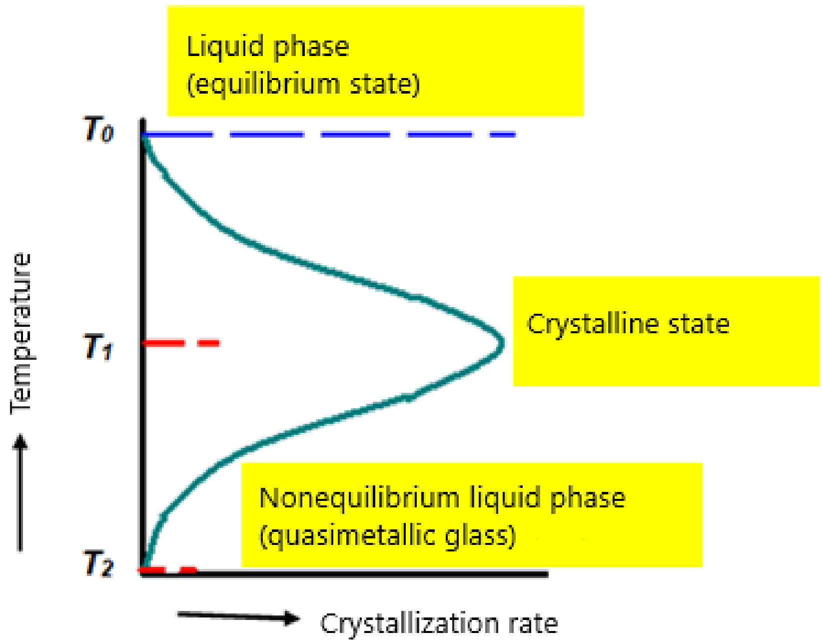

Figure 2. Temperature dependence of crystallization rate

To confirm such model, it would be advisable to conduct the following experiment: anneal the 3D sample in a wide temperature range and trace the emerging structure. If, as a result of such treatment, a characteristic structure of the annealed alloy appears the presence of equiaxed grains and wide annealing twins are detected, then it will be possible to speak of the validity of the above considerations.

In support of this version, experiments were carried out related to the thermal processing of the 3D model. For this, the smelted samples were subjected to annealing at a temperature of T = 300 °C, T = 600 °C and T = 1000 °C for 5 hours. With this treatment, one would expect a phase transition to occur – a crystallization process associated with the transition from a liquid to a crystalline state (i.e., solidification under heating conditions).

Figure 3 shows the images of microstructures after the indicated annealing modes. As can be seen, treatments at a temperature of T = 300 °C and T = 600 °C (Fig 3a and Fig. 3b) is practically not affected by the structural state of the alloy. It is typical for structures obtained directly during the fusion process. At the same time, annealing at an maximum temperature T = 1000 ° C (Fig. 3c) (solidus temperature is almost reached) leads to a significant structural change. Clear characteristics of a crystalline structure are manifested. In particular it is possible to fix the clear boundaries of the grain structure (see the inset in Fig. 3c). If based on the temperature dependence of thermodynamic and kinetic factors, during heating (as opposed to cooling), both of these parameters should act unidirectionally. It can be assumed that longer annealing at the indicated temperature T = 1000 ° C will lead to the formation of a structure whose character is fully consistent with the structure of the annealed alloy.

Thus, we can conclude that under this experiment conditions, under the selective laser smelting of the powder fractions made of the Cu81-Ni19 alloy, circumstances are created for fixing the quasi-liquid state (at least partial). As a result, a mixed structural state is formed, including a significant proportion of the amorphous structure.

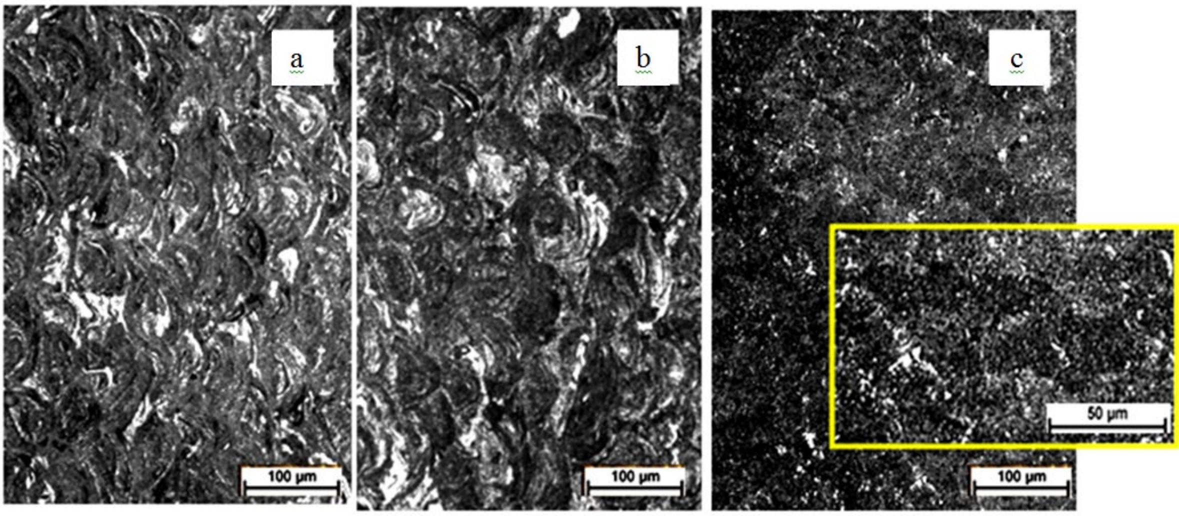

Figure 3. The microstructure of the 3D model samples made of the Cu81-Ni19 alloy after annealing at the temperature T = 300 ° C (a), T = 600 ° C (b) and T = 1000 ° C (c) for 5 hours.

The Cu81-Ni19 alloy physic and mechanical properties are determined after various technological treatments. The density ρ, roughness R_a, and microhardness $HV_{0.5}$ were determined. The results of the properties are given in table 1.

Density is an important indicator for assessing the physical condition of a material smelted from powder fractions. As a result, the following data were obtained: the density of the monolithic sample was 8.925 g/cm^3, and that of the smelted sample was 8.562 g/cm^3, i.e. the smelted material was formally less dense. However, this difference is not fundamental in nature - it is only 4%. Thus, we can conclude that the selective laser smelting method allows one to obtain an article that is almost identical in density to standard technology and, therefore, devoid of the typical disadvantages inherent in powder materials.

Table 1. The Cu81-Ni19 alloy physic and mechanical properties in the annealed state (monolith) and after selective laser smelting (3D model)

	Material characteristics		
Sample	Density ρ, g/cm^3	Roughness Ra, nm	Microhardness $HV_{0.5}$
Monolith	8,925±0,005	710±15	62±3
Laser smelted	8,562±0,005	660±20	75±3

The surface roughness parameters were evaluated. There is an inequality in the roughness values (relief profile) of the samples surface obtained by different technologies. The article obtained by laser fusion is characterized by relatively better "smoothness". The strength properties comparison allows us to conclude that the article microhardness in the initial (monolithic) state is significantly lower than the 3D sample microhardness: 62 $HV_{0.5}$ and 75 $HV_{0.5}$, respectively (the difference is more than 20%). It can be assumed that high hardness characteristics are explained by the fact that the smelted 3D sample has a predominantly amorphous structure [10-12].

4. Conclusion

Three-dimensional construction of a 3D model made by the selective laser smelting (SLS) method was implemented in relation to a copper-nickel alloy Cu81-Ni19 composition. Microstructure study has shown that the finished 3D model is not characterized by the typical features of a crystalline structure. It has been suggested that, under the conditions of the 3D model formation, the crystallization process

IOP Conf. Series: Materials Science and Engineering **971** (2020) 032053 doi:10.1088/1757-899X/971/3/032053

is suppressed. This leads to a mixed structure with an amorphous state predominance. Subsequent high-temperature annealing (T = 1000 °C) of the smelted article allows the amorphous state to be transferred to the classical crystalline position. It is shown that the density of the 3D model obtained by SLS method is almost equal to the density of the monolithic analogue, but it is significantly distinguished by a lower surface roughness and higher microhardness values.

References

[1] Sedlaka J., Rican D. Study of materials produced by powder metallurgy using classical and modern additive laser technology // Procedia Engineering. 2015. V. 100. P. 1232-1241.
[2] Yadroitsev I. Selective laser melting: Direct manufacturing of 3D-objects by selective laser melting of metal powders // Lap Lambert Acad. Publ. 2009. P.280.
[3] Herderick E. D. Additive manufacturing in the minerals, metals, and materials community: past, present, and exciting future // JOM. 2016. V. 68. № 3. P. 721-723.
[4] Barakhtin B.K., Vozniyuk A.V., Deev A.A., Zhukov A.S. Structural and mechanical state of additively sintered material under the hot plastic deformation conditions // Material deformation and fracture. 2017. № 2. P. 8-15.
[5] Gryaznov M.Yu., Shotin S.V., Chuveldiev V.N. The mesostructural hardening effect of steel 316 L grade during layer-by-layer laser smelting // Vestnik NSMU. Solid state physics. 2012. № 5. P.43-50.
[6] Zito D., Carlotto A., Loggi A., Bortolamei S., Molinary A., Cristofollini I. Latest developments in selective laser melting production of gold jewelry // The Santa Fe Symposium. 2012. P. 537-562.
[7] Louvis E. Selective laser melting o aluminium components // Journal of Materials Processing Technology. 2011. V. 211. P. 275-284.
[8] Grachev S.V., Baraz V.R., Bogatov A.A., Shveikin V.P. Physical metallurgy. Tutorial // Yekaterinburg: USTU-UPI. 2009. 548 p.
[9] Zhukov A.S., Barakhtin B.K., Vozniyuk A.V. The additive technologies using in the creation of structural materials at the nanocenter site SIC "Kurchatov Institute" - Central Research Institute of CM "Prometheus" // Materials Science. 2018. № 6. P. 11-15.
[10] Zaimovskiy V.A., Kolupatva T.L. Unusual properties of conventional metals // M.: Science, 1984. 192 p.
[11] Hanzl P., Zetek M. The influence of processing parameters on the mechanical properties of SLM parts // Procedia Engineering. 2015. V. 100. P. 1405-1413.
[12] Luzgin D.V., Polkin V.I. Properties of bulk metal glasses // Universitiy News. Non-ferrous metallurgy. 2016. № 6. P. 71-85.